One-dimensional simulation of thin liquid-film-edge retraction

Simon Čopar and Alojz Kodre
Faculty of Mathematics and Physics, University of Ljubljana, Jadranska 19, 1000 Ljubljana, Slovenia
(Received 9 August 2010; published 10 November 2010)

The phenomenon of liquid film retraction, occurring in bursting bubbles, is investigated in the simplest case of a semi-infinite sheet of inviscid liquid. Discretized equations of motion are solved on a staggered grid, with the boundary condition adapted to handle movement and breakup of liquid domain. Two independent approaches show a perfect agreement. The calculation shows a periodic pinchoff of small droplets, in contrast to the published results on viscid fluids where the liquid accumulates at the rim. A quantitative analysis of simulated liquid profiles shows that the characteristic parameters are very close to the theoretical predictions obtained from energy conservation and laws of motion.

DOI: 10.1103/PhysRevE.82.056307 PACS number(s): 47.20.Dr, 47.10.ab, 47.11.Bc

I. INTRODUCTION

In many natural phenomena involving free liquid surface, the bulk flow is strongly coupled to the dynamic boundary conditions. In extreme configurations such as jets, films, and droplets, the surface dynamics becomes dominant, and effects of surface tension play an essential role. Jets are intrinsically unstable and break apart into droplets via Rayleigh instability [1,2]. Liquid films are stable to small perturbations [1] and can be further stabilized by surfactants, with notable examples being soap bubbles and foam. When the film is punctured, the resultant free edge with a high surface curvature quickly retracts under the influence of the surface tension. This process is most easily observed in bursting soap bubbles [3]. The first experiments and theoretical predictions were made by Rayleigh at the beginning of the 20th century [4], but new findings keep being published [5–7]. Experiments [8–11] have shown that a thick rim forms at the edge and grows in time. The rim itself is unstable and leaves a trail of droplets behind it. For a finite viscosity, the rim does not detach from the film [12,13]. This results in rather large droplets, compared to the initial thickness of the film. In the limiting case of semi-infinite planar film of inviscid liquid of uniform thickness with a free edge, the number of free parameters is reduced and a clear insight into mechanics of the breakup is gained.

The problem is first investigated by means of analytical approximations and conservation laws. The predictions are compared to numerical results, obtained from a one-dimensional finite difference scheme, modified to handle the free edge correctly and stably. The interpretation of the results underlines the difference from the well-investigated viscous case.

II. THEORETICAL ESTIMATES

We assume that the breakup of the film is fully contained in a two-dimensional cross section normal to the edge, so that translational symmetry in the remaining dimension is retained. With this approximation, complex geometrical circumstances which could arise in three dimensions are eliminated. The hypothetical two-dimensional liquid breaks up into cylindrical strands, which in three-dimensional world rapidly dissolve into droplets via Rayleigh instability [1]. We also assume that the liquid is inviscid, so that energy is exactly conserved.

Assuming the breakup into two-dimensional droplets (cylinders) of roughly the same size, a relation between radius of droplets and their velocity can be derived. Initially, we have a stationary liquid sheet with width l, half-thickness h_0, and surface energy per unit of width $2l\sigma$. After breakup, all the liquid is moving with velocity v. The resulting $N=2lh_0/\pi r^2$ droplets of radius r have less surface energy than the initial film. The energy balance gives

$$\sigma N 2\pi r + 2lh_0\rho\frac{v^2}{2} = 2l\sigma. \tag{1}$$

Introducing nondimensional variables, where lengths are measured in units of h_0 and velocity in units of $v_0=\sqrt{\sigma/\rho h_0}$, we obtain a relation

$$\frac{2}{r} + \frac{v^2}{2} = 1. \tag{2}$$

In the limit of $r\to\infty$, all of the energy is in the motion. The nondimensional velocity $v=\sqrt{2}$ corresponds to the Rayleigh's result $v=\sqrt{2\sigma\rho h_0}$ [1,8]. This is the maximum velocity that the droplets can reach.

To simulate the detailed dynamics of the liquid, the equations of motion are applied. For a one-dimensional model, besides the horizontal velocity v, the half-thickness h of the film is introduced as additional variable, both dependent only on one coordinate x and time. The approximation implies that v does not vary considerably across the film thickness and that the transverse velocity is negligible. This is true for films with small variation of thickness.

Euler equation retains its form in this approximation. The continuity equation reduces to a form similar to that for compressible fluids, with h playing the role of density,

$$\frac{\partial v}{\partial t} + v\frac{\partial v}{\partial x} = -\frac{\partial p}{\partial x}, \tag{3}$$

$$\frac{\partial h}{\partial t} + \frac{\partial hv}{\partial x} = 0. \tag{4}$$

The pressure term in Euler equation is governed by the surface tension and is proportional to the surface curvature. It is an intermediate variable that only depends on the thickness profile.

The conservation of energy has yielded a relation between velocity and droplet radius. If the breakup of the film is a steady and uniform process, there must be another relation to fix the values of velocity and radius of the droplets.

A scenario of the steady-in-time droplet formation is particularly enlightening. In this case, thickness and velocity profiles retain their form in time. The motion should therefore be either periodic or uniform. The droplet formation is clearly periodic, but we can assume a uniform dynamics far from the free edge of the film. If the velocity profile is only translated with time, it automatically satisfies the advection equation. We need not know anything about the nature of the profile disturbances, only that they move with a fixed velocity c:

$$\frac{\partial v}{\partial t} + c\frac{\partial v}{\partial x} = 0. \tag{5}$$

At the edge itself, not only the disturbances are moving, but also the liquid is moving. If the liquid moved faster than the disturbances, shock waves would form and there would be no smooth and uniform movement. If the liquid moved more slowly, the deviations would outrun the liquid motion and the film would break up globally, without a clearly defined front.

The motion can be periodic only if the velocity of the formed droplets equals the speed of infinitesimal waves on the surface. Far from the edge, the linearized Euler equation applies:

$$\frac{\partial v}{\partial t} = -\frac{\partial p}{\partial x}. \tag{6}$$

Comparing Eqs. (5) and (6) gives the relation

$$p = cv. \tag{7}$$

As $c=v$ at the edge where the breakup occurs, this yields a second relation between radius and velocity. We get

$$\frac{v^2}{2} = 0.2, \quad r = 2.5. \tag{8}$$

This result is derived by purely phenomenological reasoning. Its validity is tested by numerical simulations described in the following sections. In contrast, if the rim does not detach from the film, a similar derivation gives $v^2/2=0.5$ [14].

III. DISCRETIZATION SCHEME

Numerical simulation of the breakup requires solving Euler and continuity equations [Eqs. (3) and (4)]. The basis of our algorithm is an equidistant finite difference grid. Since for Euler equation a scheme with all variables defined at the same nodes is not stable [15], we use a staggered grid scheme, where velocity nodes are shifted for half a grid spacing with respect to thickness and pressure nodes (Fig. 1). The discretization of the required spatial derivatives involves three adjacent nodes. Symmetric central differences are used for simple derivatives. The product terms are discretized with formulas, adjusted to match the exact expressions to the highest possible order in Taylor expansion [16]:

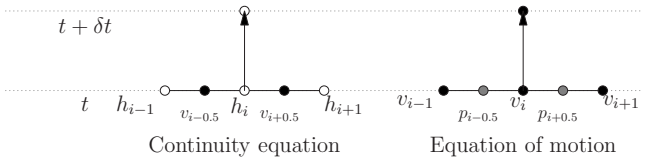

FIG. 1. Explicit discretization scheme for Euler and the continuity equation on the staggered grid. Velocity nodes are shifted with respect to thickness and pressure nodes.

$$\left(v\frac{\partial v}{\partial x}\right)_i = \frac{1}{2\delta x} v_i (v_{i+1} - v_{i-1}), \tag{9}$$

$$\left(\frac{\partial vh}{\partial x}\right)_i = \frac{1}{2\delta x}[v_{i+1/2}h_{i+1} - v_{i-1/2}h_{i-1} + h_i(v_{i+1/2} - v_{i-1/2})]. \tag{10}$$

The handling of boundary conditions will require a time-explicit scheme. Nodes, used to make a time step for each equation, are shown in Fig. 1.

The continuity equation [Eq. (4)] is modified by a surface-smoothing dissipation term, which ensures stability of the scheme,

$$\frac{\partial h}{\partial t} + \frac{\partial hv}{\partial x} = \eta\frac{\partial^2 h}{\partial x^2}. \tag{11}$$

The second derivative of the thickness provides a diffusion-like effect and conserves the volume. Conservation of energy in the original equation, however, results in marginally unstable numerical scheme and the additional term shifts the balance just enough to cancel out the effects of discrete grid. According to von Neumann analysis [16], values higher than $\eta > 64\delta t^3/\delta x^6$ are needed for the purpose. In the simulations, smaller values can be used, relying on nonlinear effects and boundary conditions to provide the necessary stabilization.

For pressure, the exact three-point formula for curvature is used, to yield correct behavior at the edge, where the slope of the surface is significant,

$$p = -\frac{D^2 h}{\sqrt{1+(D_+h)^2}\sqrt{1+(D_-h)^2}\sqrt{1+(D_0h)^2}}. \tag{12}$$

Subscribed symbols D in the denominator stand for right, left, and central first differences, respectively, and D^2 is the central second difference.

IV. FLOATING BOUNDARY CONDITIONS

The main concern of our numerical experiment is a scheme, capable of handling droplet separation and joining.

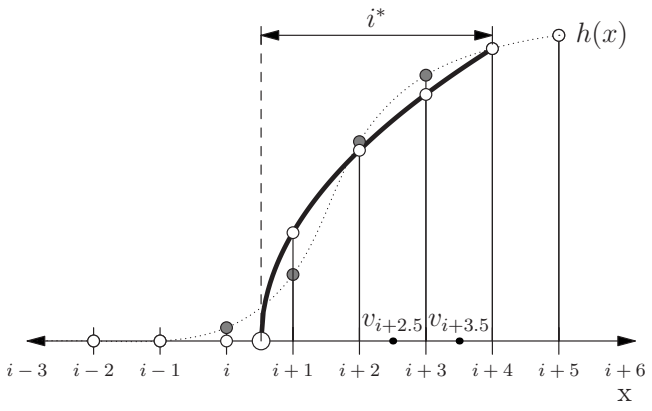

FIG. 2. Edge handling for the parabolic approximation approach. In each time step, h values at four edge nodes are replaced with a square-root function with equivalent volume, and the velocity is set to the average of two marked nodes.

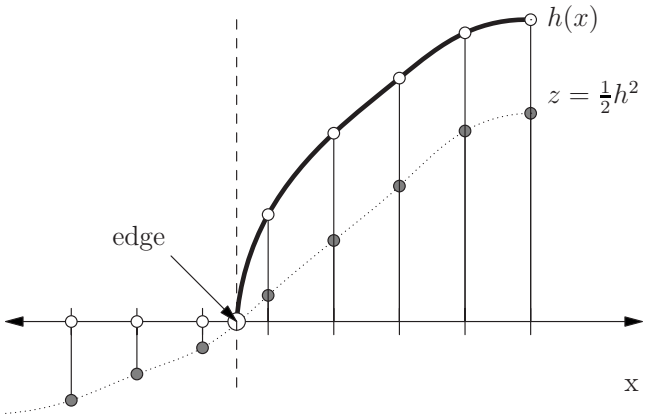

FIG. 3. Edge handling for the regularization approach. Variable z is regular everywhere, and the edge singularity only shows when we extract the thickness profile.

In these processes, the domain, occupied by the liquid, changes in time and is not simply connected. Dynamic grids or two-component computational fluid dynamics schemes like *volume of fluid* algorithm [17] are routinely used for this purpose.

As the problem is one dimensional, there is no need to use complicated and programming-intensive methods. Instead, we modify the staggered grid evolution by including an additional step that handles free edges in a physically correct way.

Surface tension ensures that the surface of the film is smooth everywhere, even at the edge. The edge has approximately cylindrical shape with a vertical tangent, where the discretization of thickness derivatives ultimately fails for any grid resolution. An additional problem arises with pressure calculation. Three-point formula should be applied to three adjacent nodes on the surface, but the nodes outside the edge are not part of the liquid. Moreover, the edge position uncertainty equals the grid spacing.

We solve the problem by a separate treatment of the liquid at free edges. Two different approaches to the problem are described below.

A. Parabolic edge

The shape of the surface at the edge can be approximated by a circular arc or, rather, a square-root parabola. As the discretization scheme fails at the edge, we adopt an approximate edge position by finding the first nonzero thickness node. The thickness values at the last four nodes are then replaced with those from an analytical expression of a square-root parabola with the same volume and width (Fig. 2). The velocities are averaged and the pressure at the edge is expressed by the parameters of the parabola (for the definition of used symbols, see Fig. 2),

$$p = \frac{2i^* \delta x}{h_{i+4}^2}. \tag{13}$$

This replacement has the same effect as a very fast relaxation of the edge to the static equilibrium shape, disregarding the interaction with other parts of the film.

The nodes outside the fluid domain are set to $h=0$ and are skipped in the calculation of the next time step. This is the reason why time-implicit schemes cannot be used.

B. Regularization variable

Another way of handling the singularity at the edge is substitution of a new variable. The thickness h behaves as a square root at the edge, so the new variable

$$z = \tfrac{1}{2}h^2 \tag{14}$$

is regular everywhere and behaves linearly at the edge. Negative values can be assigned to the parts without the liquid. In retrieving h, the square root reproduces the root-type singularity and removes negative parts (Fig. 3).

As thickness is not present in Euler equation, the substitution only affects the continuity equation, which gets an additional term,

$$\frac{\partial z}{\partial t} + \frac{\partial z v}{\partial x} + z\frac{\partial v}{\partial x} = 0. \tag{15}$$

The pressure formula transforms into

$$p = -\frac{2z\dfrac{\partial^2 z}{\partial x^2} - \left(\dfrac{\partial z}{\partial x}\right)^2}{\left[2z + \left(\dfrac{\partial z}{\partial x}\right)^2\right]^{3/2}}. \tag{16}$$

This expression is defined on a larger domain than the original. It is also smooth at the edge, which eliminates the numerical problems.

With the regularized edge, we have to ensure that z is tame in the negative part. There is no need to calculate pressure there, but we need to ensure that z does not pop back into the positive domain and that it remains smooth enough, not to disturb the positive parts via interaction through the edge.

This is ensured by using a different dynamics for the negative part,

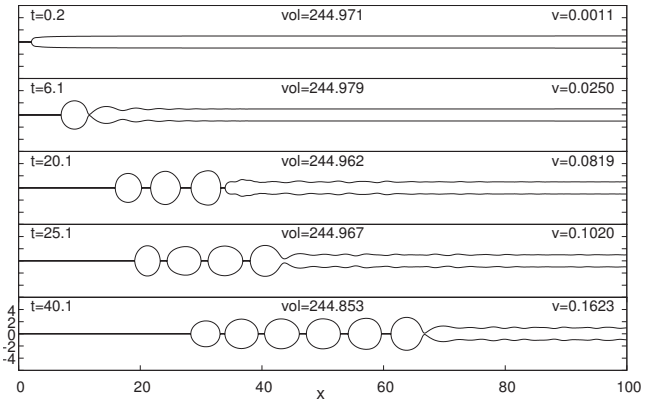

FIG. 4. Thickness profile at different times, given by numerical simulation. We can see periodic droplet pinchoff, the motion of individual droplets, and their vibrations. Labels show simulation time, current volume, and average velocity.

$$\frac{\partial z}{\partial t} = \beta \frac{\partial^2 z}{\partial x^2} - \psi. \tag{17}$$

The first term ensures the smoothness and the second part ensures negativity. By trial and error, the parameters are set to $\beta = 0.005\ 25$ and $\psi = 5\beta$.

The advantage of this approach over the parabolic approximation is in the local treatment, with the only modification that the equation for z depends on its sign. As there is no stitching of different functions, the results are smoother, with fewer residual shocklike disturbances.

V. RESULTS AND COMPARISON

The initial state of the simulation is set to a stationary planar film of uniform thickness $h=1$, with a free edge on the left. The parameters are fixed to

$$\delta x = 0.05, \quad \delta t = 0.0005, \quad \eta = 0.025. \tag{18}$$

Fine tuning of parameters such as the node weights in velocity-averaging and negative-z parameter ψ is performed to optimize volume and energy conservation and to improve stability in worst-case initial conditions.

After tuning, both approaches give the same results. Not only is the qualitative behavior similar, but also the results stay in a very good synchrony for longer periods of time.

The time evolution of the height profile, as seen in Fig. 4, shows that the fluid film breaks apart into two-dimensional droplets in uniform time intervals and that the droplets are uniform in size. On average, they are perfectly circular, owing to the exact expression for curvature. The waves further along the film move with the same velocity as the droplets, exactly like predicted in analytical estimates. Despite the one-dimensional approximation, the droplets show realistic quadrupolar vibrations after the breakoff (compare frames in Fig. 4).

Velocity and pressure profiles stay in phase for the entire interval of computation (Fig. 5), confirming the proportionality $p = cv$, predicted by the linear wave approximation [Eq. (7)]. The two approaches differ in the smoothness of

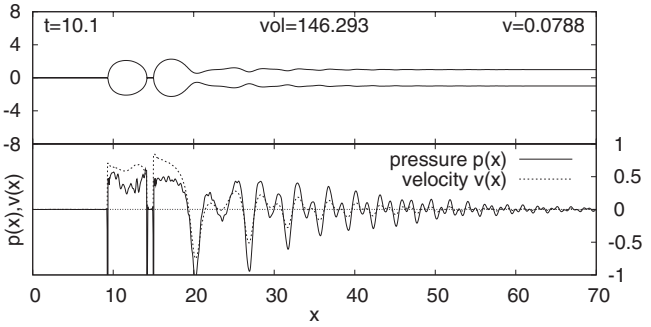

FIG. 5. Comparison of pressure and velocity profiles on the same scale shows that they are in phase, which is in agreement with the approximate proportionality, predicted by comparing wave and Euler equations [Eq. (7)].

pressure profile: the parabolic edge approach shows high-frequency noise around the edge, a consequence of stitching the parabolic segment to the numerical data (Fig. 6).

The average droplet velocity and radius, obtained from both methods are in very good agreement with the analytical prediction [Eq. (8)]. Their compliance with energy conservation [Eq. (2)] can be checked by comparing the left-hand side of the equation with the exact value:

	Simulation	Theory
v	0.62 ± 0.01	0.632
r	2.65 ± 0.01	2.5
$\frac{2}{r} + \frac{v^2}{2}$	0.947	1

The 5% energy loss is mostly due to droplet oscillation. The momentum of the entire body of fluid grows linearly in time:

$$\langle v \rangle = at, \quad a = 0.004\ 06. \tag{19}$$

Newton's law for the given volume of fluid (490 for this simulation) yields the force $F = Vd\langle v \rangle / dt = Va = 1.989$. This

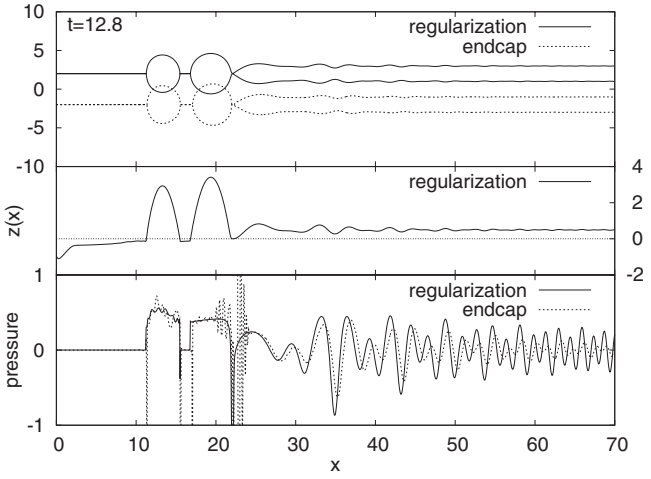

FIG. 6. Comparison of both numerical approaches. Regularization approach gives a smoother pressure profile and is less prone to high-frequency instabilities seen on the profile given by the parabolic endcap approach.

result is justified by a simple reasoning. At the edge, a pressure of $p=1/r$ acts on the widest cross section of the forming droplet with diameter $2r$. The resulting force is $F=2rp=2$, which is almost exactly the result given by simulation.

VI. CONCLUSION

We present two simple one-dimensional approaches for evolving dynamics of a thin liquid film with a free edge, leading to tearing and breaking of the film. Both approaches are based on the basic staggered grid scheme, with added steps for edge handling. The methods perform extremely well by criteria of energy and volume conservation, as well as consistency of results in intercomparison.

The methods are used to investigate droplet formation at the free edge of the liquid film, with encouraging results. Our results reproduce the crude analytical estimations to a few percent, which leads to a conclusion that the breakup is a robust process and mostly independent of exact hydrodynamic details.

Past simulations have shown [12,13] that in the presence of finite viscosity, there is no droplet formation on the small scale; instead, a thick rim of fluid forms at the retracting edge, breaking up eventually into large and fast droplets. Our calculations and simulations show that in the inviscid case the breakup occurs uniformly and periodically, forming small droplets, comparable to the film thickness. Droplet formation is a borderline process, and a small viscous term is enough to prevent the droplet pinchoff. Low-viscosity profiles computed by Zavaleta [13] resemble our profiles away from the edge, but the droplets fail to detach.

The method can be applied to the viscous case, although multiple-edge handling is not so important in that case, as the breakup into droplets is less likely. It can be extended to cylindrical geometry, e.g., to reproduce the Rayleigh instability. The substitution method has some potential for extension into two dimensions. Our contribution gives an insight into the mechanics of droplet formation and phenomenological descriptions lying behind the propagation of a free liquid edge.

[1] P. G. Drazin, *Introduction to Hydrodynamic Stability* (Cambridge University Press, Cambridge, England, 2002).

[2] J. Eggers and E. Villermaux, Rep. Prog. Phys. **71**, 036601 (2008).

[3] G. Rämme, Phys. Educ. **24**, 147 (1989).

[4] L. Rayleigh, *Scientific Papers 3* (Cambridge University Press, Cambridge, England, 1902), p. 441.

[5] J. C. Bird, R. de Ruiter, L. Courbin, and H. A. Stone, Nature (London) **465**, 759 (2010).

[6] R. V. Craster and O. K. Matar, Rev. Mod. Phys. **81**, 1131 (2009).

[7] H. Lhuissier and E. Villermaux, Phys. Rev. Lett. **103**, 054501 (2009).

[8] A. B. Pandit and J. F. Davidson, J. Fluid Mech. **212**, 11 (1990).

[9] G. Taylor, Proc. R. Soc. London, Ser. A **253**, 313 (1959).

[10] F. Müller, U. Kornek, and R. Stannarius, Phys. Rev. E **75**, 065302(R) (2007).

[11] E. Reyssat and D. Quéré, EPL **76**, 236 (2006).

[12] G. Sünderhauf, H. Raszillier, and F. Durst, Phys. Fluids **14**, 198 (2002).

[13] L. J. G. Zavaleta, *Self-Similar and Traveling Wave Solutions in Surface Tension-Driven Thin Planar Flims*, Tech. Rep. (Scientific Computing Advanced Training, 2007).

[14] F. E. C. Culick, J. Appl. Phys. **31**, 1128 (1960).

[15] K. A. Hoffmann, *Computational Fluid Dynamics* (Engineering Education System, Wichita, Kansas, 2000), Vol. 1.

[16] C. A. J. Fletcher, *Computational Techniques for Fluid Dynamics* (Springer-Verlag, Berlin, 1991), Vol. 1.

[17] C. A. J. Fletcher, *Computational Techniques for Fluid Dynamics* (Springer-Verlag, Berlin, 1991), Vol. 2.